Journal of Magnetic Resonance **145,** 237–245 (2000)
doi:10.1006/jmre.2000.2086, available online at http://www.idealibrary.com on IDEAL®

Single-Quantum Coherence Filter for Strongly Coupled Spin Systems for Localized ^{1}H NMR Spectroscopy

Andreas H. Trabesinger, D. Christoph Mueller, and Peter Boesiger

Institute of Biomedical Engineering and Medical Informatics, University of Zurich and Swiss Federal Institute of Technology, CH-8092 Zurich, Switzerland

Received November 2, 1999; revised March 23, 2000

A pulse sequence for localized *in vivo* ^{1}H NMR spectroscopy is presented, which selectively filters single-quantum coherence built up by strongly coupled spin systems. Uncoupled and weakly coupled spin systems do not contribute to the signal output. Analytical calculations using a product operator description of the strongly coupled AB spin system as well as *in vitro* tests demonstrate that the proposed filter produces a signal output for a strongly coupled AB spin system, whereas the resonances of a weakly coupled AX spin system and of uncoupled spins are widely suppressed. As a potential application, the detection of the strongly coupled AA′BB′ spin system of taurine at 1.5 T is discussed.

Key Words: **single-quantum coherence; strong coupling; weak coupling; brain.**

INTRODUCTION

The number of metabolites that may be unequivocally identified in conventional *in vivo* ^{1}H NMR spectra of brain tissue acquired on clinical scanners with field strengths of 1.5 T is quite small compared with the considerably larger number of small molecules that contribute to the proton spectra. Problems arise from low metabolite concentrations in brain tissue (<10 mmol/L) as well as from spectral overlap of resonance lines. The latter fact stems from the small dispersion of the NMR signals of carbon-bound hydrogen nuclei ($\sim$300 Hz at 1.5 T) in combination with spectral linewidths of >1 Hz caused by the rather poor field homogeneity of whole-body NMR spectrometers.

Spatial localization is a prerequisite that pulse sequences for *in vivo* use have to fulfill. Most ^{1}H *in vivo* MR spectroscopy sequences employ pulsed field gradients in combination with at least three spatially selective RF pulses for this task. Due to spin evolution in the delays in between the pulses, signals of spin systems with active couplings will usually appear as *J*-modulated multiplets, e.g., in PRESS (*1*) or STEAM (*2*) spectra. Strong coupling between hydrogen nuclei lead to complicated spectral patterns and thus to a still more difficult spectral assignment of the detected resonances.

An alternative to acquiring the entire proton spectrum of the sample under investigation is the use of metabolite-specific pulse sequences (*3*). They make use of a specific network of *J*-coupling and chemical shift values to label spin systems whose signal should be selectively detected, whereas the signal from all other spin systems (or at least of those resonating in the same spectral region) should be suppressed. Among various techniques, multiple-quantum coherence (MQC) filtering sequences are increasingly applied on clinical scanners for the selective detection of human brain metabolites (*4–10*). The concept of MQC filtering promises good background discrimination, in particular against uncoupled spin systems. In addition, several approaches have been proposed during the past decade to combine the filtering section with spatial localization procedures to a single-shot method (*4, 5, 11–15*) leading to small susceptibility to patient movement. On the other side, as the intensity of the MQC filtered spectrum depends on the number of transitions contributing to it, MQC filtering sequences suffer from inherent signal loss, which is often too high to allow the detection of low concentrated metabolites in the brain.

Single-quantum coherence (SQC) filtering has promising features for *in vivo* applications, especially promising signal yield. On the other hand, SQC filtering has disadvantageous properties of its own that must be taken care of with precaution. In particular, every spin system—including uncoupled spins—potentially contributes to the SQC filtered signal.

In this report, a spatially fully localized SQC filtering sequence is presented, which inherently suppresses signals arising from uncoupled and weakly coupled spins, but yields signal for strongly coupled spins. This feature is particularly interesting for low and medium fields, which are used for *in vivo* experiments on humans and animals. The usefulness of the proposed sequence for *in vivo* applications is exemplified for the strongly coupled taurine AA′BB′ spin system.

MATERIAL AND METHODS

SQC Filtering Sequence

Multiple-quantum transitions are generally detected indirectly in a three-step process (cf. Fig. 1), consisting of (a) excitation of MQC, (b) their free evolution, and (c) conversion

1090-7807/00 $35.00

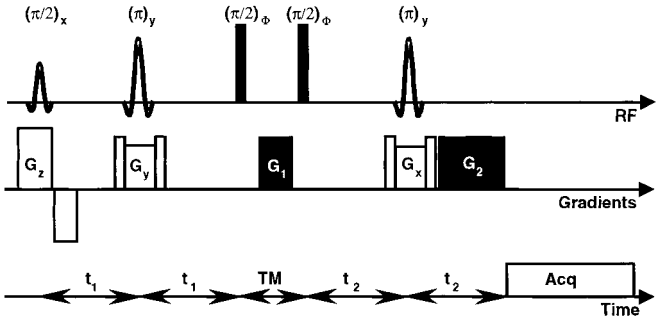

FIG. 1. Volume-selective multiple-quantum coherence (MQC) filtering sequence. $\phi = x$ for even MQC orders, $\phi = y$ for odd MQC orders.

into observable single-quantum coherence (*16*). Excitation of MQC is usually achieved using the pulse sandwich $[(\pi/2)_x$–t_1–$(\pi)_y$–t_1–$(\pi/2)_\phi]$, with $\phi = x$ if even orders of MQC should be excited and $\phi = y$ for odd MQC orders. After a free evolution period TM, a $[(\pi/2)_\phi$–t_2–$(\pi)_y$–$t_2]$ sequence creates single-quantum antiphase coherence and allows it to be converted into in-phase coherence, which is subsequently detected. To specifically select coherence of order n, coherence pathway filtering with static field gradients (*17*) may be applied by inserting two filter gradients G_1 and $G_2 = n \cdot G_1$ (cf. Fig. 1). In this way, the method becomes a genuine single-shot technique as opposed to methods employing phase cycling for the selection of specific MQC orders.

Localization properties are introduced into the sequence by making the initial $(\pi/2)$ pulse and the two refocusing pulses slice selective, in analogy to the PRESS localization sequence (*1*). These three pulses are appropriate for localization purposes as they play a null role in coherence transfer. We use optimized sinc-Gauss pulses. The additional $(\pi/2)$ pulses are block pulses.

For SQC filtering (cf. Fig. 2), the pulse sequence may be simplified, as the single-quantum coherence built up by the second $(\pi/2)$ pulse is already detectable. Therefore, the third $(\pi/2)$ pulse may be skipped and, in addition, the filtering gradients may be abandoned as the MQC orders $\neq 1$ are not detectable and thus need not be dephased.

As at least n coupled spins $\frac{1}{2}$ are necessary to form a n-quantum transition, coherence order is limited by the number of spins in the spin system. Thus a MQC filter may be regarded as a high pass filter in the spin number domain. From this point of view, all spins potentially contribute to the SQC filtered signal.

The above-mentioned choice of the phase of the second $(\pi/2)$ pulse (i.e., $\phi = x$ for even MQC orders, $\phi = y$ for odd MQC orders) is motivated by calculations made for weakly coupled spin systems (*16, 18*). In the following discussion, not only weakly coupled spins (with the special case of uncoupled spins), but also strongly coupled spins shall be treated. When dealing with strongly coupled spin systems, phase settings, which differ from the ones conventionally chosen, may also lead to excitations of MQC of the desired order. In the following, the effect of the sequence depicted in Fig. 2 with ϕ set to x (instead of y) is analyzed.

For the analysis of *weakly coupled (and uncoupled) spins*, a product operator description (*18–20*) is employed. We adapt the convention of positive rotation in the right-handed sense (*18*). Without the restriction of generality we treat the case of a spin A imbedded in an AX_n spin system, i.e., one spin which is weakly coupled to n magnetically equivalent spins ($n = 0$ for uncoupled spins). The weak coupling condition demands for $|J_{AX}| \ll |\nu_A - \nu_X|$. After the $(\pi/2)_x$ excitation pulse (cf. Fig. 2), the A spin density matrix, which initially described thermal equilibrium magnetization, has evolved into

$$\rho(0^+) = -A_y. \qquad [1]$$

During the following spin-echo period $0^+ < t < 2t_1^-$, the linear Zeeman interaction shows no net effect; therefore, the only modulation is due to the bilinear J-coupling interaction:

$$\begin{aligned}\rho(2t_1^-) = &-A_y\cos^n(2\pi J_{AX}t_1)\\ &+ 2A_xX_z\cos^{n-1}(2\pi J_{AX}t_1)\sin(2\pi J_{AX}t_1)\\ &+ \text{terms containing more than one}\\ &\quad\text{longitudinal single spin operator.}\end{aligned} \qquad [2]$$

$\rho(2t_1^-)$ is a superposition of basis product operators of the form $2^mA_\varphi \prod_{l=1}^m X_{lz}$, $0 \le m \le n$, $\varphi = x$ for odd m and $\varphi = y$ for even m.

The subsequent $(\pi/2)_x$ pulse at $t = 2t_1$ has the following effect on the products appearing in $\rho(2t_1^-)$:

$$2^mA_\varphi \prod_{l=1}^m X_{lz} \xrightarrow{(\pi/2)_x} (-2)^mA_\xi \prod_{l=1}^m X_{ly}, \qquad [3]$$

$0 \le m \le n$, $\xi = x$ for odd m and $\xi = z$ for even m.

From [3] it becomes evident that $\rho(2t_1^+)$ contains only

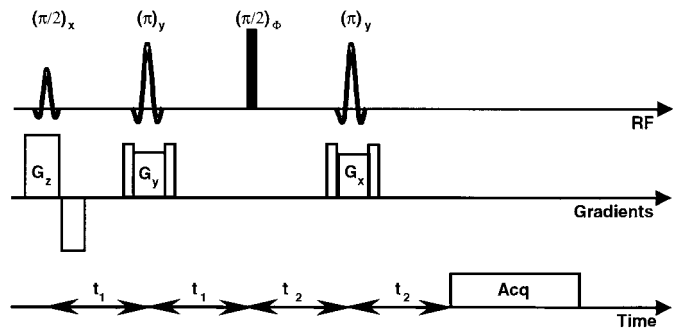

FIG. 2. Volume-selective single-quantum coherence (SQC) filtering sequence. $\phi = x$.

z-magnetization of spin A (for $m = 0$) and product operators with an even number of transversal single spin operators. Expressing the latter in terms of shifting operators,

$$I_k^{\pm} = I_{kx} \pm iI_{ky} \qquad [4]$$

shows that all product operators in $\rho(2t_1^+)$ are of an even coherence order, as each operator I_x and I_y is a linear combination of raising and lowering operators and thus the number of raising minus the number of lowering operators is even in each product appearing in $\rho(2t_1^+)$. During the following periods of free evolution, the coherence order is preserved. The only RF pulse left before acquisition is a (π) refocusing pulse at $t = 2t_1 + t_2$, which does not change the modulus of the coherence order. This means that during acquisition the density matrix contains only longitudinal spin order and even coherence orders, all of which are not directly observable. The output of the SQC filter is therefore expected to contain no signal arising from uncoupled and from weakly coupled spins.

The general analysis of *strongly coupled spin systems* is considerably more complicated. Therefore we shall restrict the discussion to the simplest case of the AB spin system of two strongly coupled spins $\frac{1}{2}$, which gives an insight into the basic mechanism that leads to observable magnetization at the beginning of the acquisition period.

The Hamiltonian generating the time evolution of a strongly coupled AB spin system during free evolution writes as

$$H = \omega_A\mathbf{A} + \omega_B\mathbf{B} + 2\pi J_{AB}\mathbf{AB}. \qquad [5]$$

Expanding the scalar product in Eq. [5] results in

$$\mathbf{AB} = A_zB_z + A_xB_x + A_yB_y. \qquad [6]$$

Extracting from Eq. [6] the bilinear rotations with transverse components (which are neglected in the weak coupling approximation) and writing them in terms of shifting operators (cf. Eq. [4]) yields

$$A_xB_x + A_yB_y = \tfrac{1}{2}(A^+B^- + A^-B^+). \qquad [7]$$

From Eq. [7] it becomes clear that during free evolution a (periodical) magnetization transfer between the strongly coupled spins takes place, yet under conservation of the coherence order. Under the (π) refocusing pulse, the modulus of the coherence order is conserved. Starting from

$$\rho(0^+) = -A_y \qquad [8]$$

(only spin A considered), exactly one spin operator in each term of the density matrix is transversal during $0^+ \le t \le 2t_1^-$.

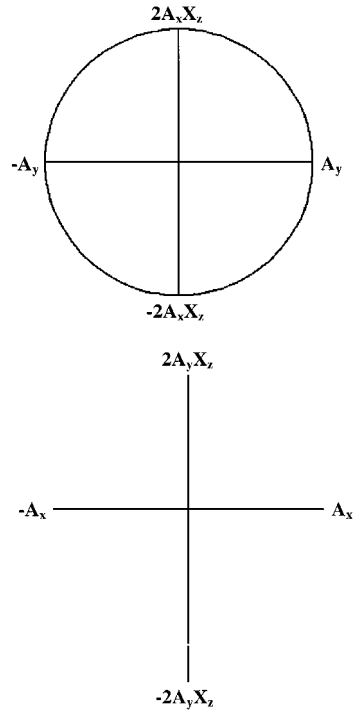

FIG. 3. Projection of the density matrix describing an ideal weakly coupled AX spin system after a spin echo experiment. Echo times range from 0 to $2/J$ ($\rho(\mathrm{TE} = 0) = -A_y$). Only the four operators containing transversal A spin magnetization are shown.

Thus, exactly four types of transversal magnetization are potentially present in the density operator $\rho(t)$ at each time: A_x, A_y, A_xB_z, A_yB_z.

In the case of a weakly coupled spin system, the net effect of a spin echo (i.e., for $\rho(2t_1^-)$) is a rotation exclusively in the $[A_y, 2A_xX_z]$ plane of the Liouville space (only spin A considered, cf. Eq. [2]), i.e., a rotation about $2A_zX_z$ (cf. Eq. [6]; the bilinear rotations with transverse components are neglected). Figure 3 shows projections of the trajectory of the density matrix onto the $[A_y, 2A_xX_z]$ and the $[A_x, 2A_yX_z]$ planes for increasing echo times $\mathrm{TE} = 2t_1$. As expected, the magnetization remains in the $[A_y, 2A_xX_z]$ plane for all echo times (cf. Fig. 6 in Ref. (*18*)). In the presence of strong coupling, components in the $[A_x, 2A_yB_z]$ plane are also mixed in, equivalent to the appearance of product operators of the form A_x and $2A_yB_z$ in $\rho(2t_1^-)$. This is demonstrated in Fig. 4, which shows the same projections as Fig. 3 for the strongly coupled citrate AB spin system in a field of 1.5 T ($\Delta\nu = 8.4$ Hz, $J = 15.4$ Hz). The calculations are based on the product operator description of the AB spin system given by Kay and McClung (*21*). The two projections show clearly the periodic appearance of terms of the form A_x and $2A_yB_z$ as the echo time is increased.

The transformation of the product operators A_x and $2A_yB_z$ under the $(\pi/2)_x$ pulse at $t = 2t_1$ is according to

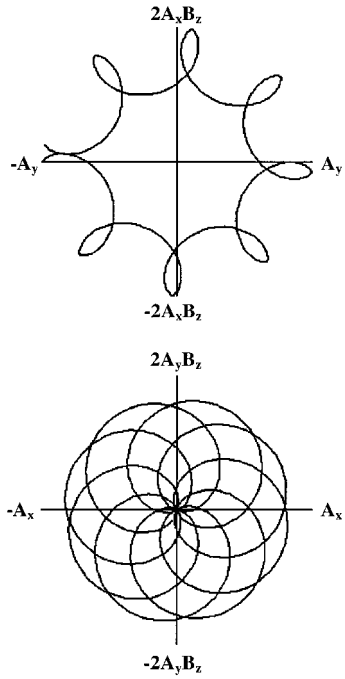

FIG. 4. Projection of the density matrix describing the strongly coupled AB spin system of citrate ($\Delta\nu$ = 8.4 Hz, J = 15.4 Hz) after a spin echo experiment. Echo times range from 0 to 900 ms $\approx 14/J$ ($\rho(\mathrm{TE}=0) = -A_y$). Only the four operators containing transversal A spin magnetization are shown.

$$A_x \xrightarrow{(\pi/2)_x} A_x$$

$$2A_yB_z \xrightarrow{(\pi/2)_x} -2A_zB_y. \qquad [9]$$

The terms A_x and $2A_zB_y$ in $\rho(2t_1^+)$ are of coherence order ± 1 and will thus lead to observable magnetization during the acquisition period.

Figure 5 shows the same trajectories as those in Figs. 3 and 4 for the 2,4-dichloropyrimidine AX spin system in a field of 1.5 T ($\Delta\nu$ = 63.3 Hz, J = 5.6 Hz). This spin system behaves nearly like an idealized weakly coupled spin system (cf. Fig. 3), but still shows some small deviations, which manifest themselves in the appearance of terms A_x and $2A_zB_y$ in $\rho(2t_1^+)$.

Phase Calibration

As apparent from the discussion given above, the two (π/2) pulses must induce exactly the same flip axis for proper working of the proposed sequence. When the volume of interest (VOI) is located outside the isocenter, the slice-selective RF pulses of the SQC filtering sequence (cf. Fig. 1) normally have nonzero frequency offsets. This leads to phase accumulation during the switching of the synthesizer frequency and therefore to a dependence of the relative phase between the first two (π/2) pulses on the location of the VOI (*6, 7*). If not accounted for, these phase shifts not only lead to a malfunctioning of the SQC filter but also impede intra- and interindividual comparability between spectra taken in different spatial locations. To avoid these drawbacks, we modified a calibration procedure proposed by Keltner *et al.* (*7*) to ensure that both (π/2) pulses invoke rotations around the same flip axis. A detailed description of the calibration procedure is given in (*10*).

EXPERIMENTAL

The sequence as summarized in Fig. 2 was implemented on a 1.5 T Philips Gyroscan ACS NT whole-body scanner equipped with a transmit/receive birdcage resonator (Philips Medical Systems, Best, The Netherlands) and a gradient coil set, providing three perpendicular gradient fields (maximal strength: 21 mT/m, maximal slew rate: 100 mT/(m · ms)).

The specificity of the proposed sequence for strongly coupled spin systems was evaluated using phantoms containing

(a) ~10 mmol/L 2,4-dichloropyrimidine (weakly coupled AX spin system),

(b) 100 mmol/L trilithium citrate (strongly coupled AB spin system),

(c) a mixture of 100 mmol/L trilithium citrate (strongly coupled AB spin system), 100 mmol/L alanine (weakly coupled AX_3 spin system), and 100 mmol/L creatine (consisting of an uncoupled A_2 and an uncoupled A_3 spin system).

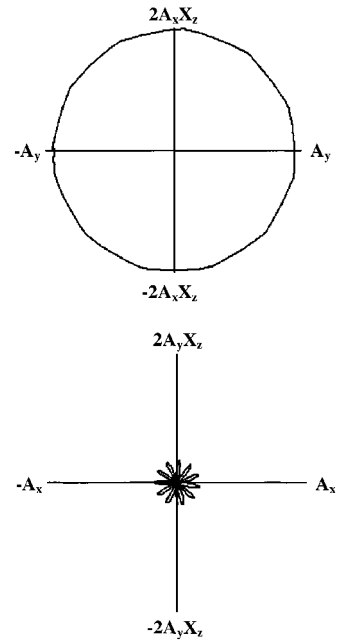

FIG. 5. Projection of the density matrix describing the weakly coupled AX spin system of 2,4-dicholropyrimidine ($\Delta\nu$ = 63.3 Hz, J = 5.6 Hz) after a spin echo for echo times ranging from 0 to 360 ms $\approx 2/J$ ($\rho(\mathrm{TE}=0) = -A_y$). Only the four operators containing transversal A spin magnetization are shown.

In addition to experiments with these model systems, we studied the behavior of taurine, a metabolite of considerable importance in biochemistry (*22*, *23*), under the proposed sequence. A phantom containing a 100 mmol/L solution was used. Taurine (2-aminoethanesulfonic acid) forms a strongly coupled AA′BB′ spin system. Its resonances appear at physiological pH at 3.27 ppm ($N–CH_2$) and 3.43 ppm ($S–CH_2$), i.e., $\Delta\nu = 10.2$ Hz at 1.5 T. The A and B spins are scalarly coupled with $J = 6.4$ Hz. In ^{1}H NMR spectra of brain tissue, the taurine resonances are overlapped by the singlet assigned to choline containing compounds at 3.23 ppm as well as by the signal of the *myo*-inositol [5]methine and [1,3]methine compounds at 3.28 and 3.54 ppm. *Myo*-inositol forms a strongly coupled AMM′NN′X spin system. In order to estimate the contamination of the taurine peak in SQC filtered spectra with interfering signals, SQC filtered spectra of taurine, choline and *myo*-inositol (each in 100 mmol/L solutions) were compared.

In order to demonstrate spatial selectivity of the proposed sequence, its localization properties were compared with those of a standard PRESS sequence (*1*). A two-chamber Plexiglas phantom was used, consisting of a cylindrical bath (inner diameter 137 mm, filled up to a height of 93 mm), in the center of which a cuboid (inner dimensions: 40 mm × 29 mm × 29 mm) was placed. Four walls of the cuboid are made of Plexiglas and two of plastic foil (cf. Fig. 9). The inner compartment was filled with a 100 mmol/L solution of ethanol (A_2X_3 spin system, $J = 7.3$ Hz); the outer compartment contained a 100 mmol/L solution of alanine (AX_3 spin system, $J = 7.3$ Hz). A volume of interest comprising $(26\ \text{mm})^3$ was chosen according to Fig. 8. Spectra were acquired using either an asymmetric PRESS sequence ($TE = 2/J = 272$ ms) or the sequence depicted in Fig. 2 with $\phi = y$ ($t_1 = t_2 = 1/2J = 68$ ms, resulting in a total sequence duration of 272 ms). The latter sequence has the same localization properties as the proposed SQC filter (where $\phi = x$), as it has to be shown that the additional $(\pi/2)$ pulse does not cause contamination of the signal with contributions from outside the nominal VOI. With the chosen timing, the X spins will be in phase along y at $t = 2t_1 = 136$ ms. Therefore, the $(\pi/2)_y$ pulse at $t = 2t_1$ does not affect the spins inside the VOI, but those in the outer compartment. If the sequence depicted in Fig. 2 was used with $\phi = x$ (i.e., the proposed SQC filter), the signals of both weakly coupled spin systems would have been suppressed. In both the PRESS and the $[(\pi/2)_x–\tau–(\pi)_y–\tau–(\pi/2)_y–\tau–(\pi)_y–\tau–$acquire] sequence, the third slice selection gradient (cf. Fig. 2) was chosen such that the selected slice includes the two walls of the cuboid that are made of foil.

FIG. 6. Spectra of the 2,4-dichloropyrimidine AX spin system. Only the signal of the A spin is shown. From left to right: PRESS spectrum (TE = 30 ms), SQC filtered spectra ($t_1 = t_2 = \tau$; $TE = 4\tau = 60$, 80, 100, 120, 140 ms).

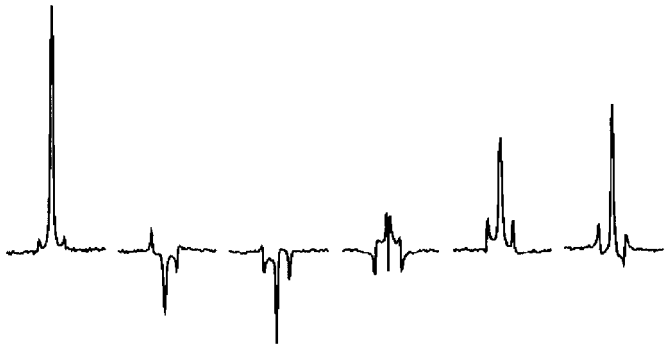

FIG. 7. Spectra of the trilithium citrate AB spin system. From left to right: PRESS spectrum (TE = 30 ms), SQC filtered spectra ($t_1 = t_2 = \tau$; $TE = 4\tau =$ 60, 80, 100, 120, 140 ms).

In all experiments, 32 measurements, which were preceded by 4 dummy excitations, were averaged at a repetition rate of 2000 ms (except for the phantom containing 2,4-dichloropyrimidine, where 128 measurements were averaged). A total of 2048 complex data points were acquired at a sampling frequency of 2000 Hz. If not stated differently, the VOI comprised $(25\ \text{mm})^3$. All spectra were acquired using a phase cycling scheme, which integrates the phase of the additional $(\pi/2)$ pulse into an extended 16-step "exor-

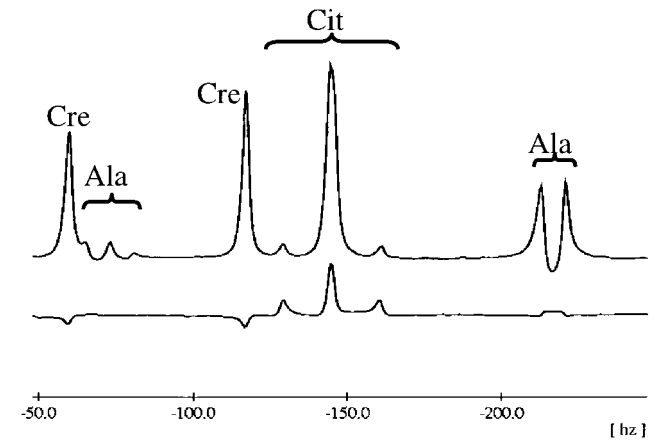

FIG. 8. Spectra of a mixture of 100 mmol/L trilithium citrate (strongly coupled AB spin system), 100 mmol/L alanine (weakly coupled AX_3 spin system), and 100 mmol/L creatine (uncoupled A_2 and uncoupled A_3 spin system). Top: PRESS spectrum (TE = 30 ms), bottom: SQC filtered spectra ($t_1 = t_2 = \tau$; $TE = 4\tau = 80$ ms). Note that the SQC filtered spectrum is 180° phase shifted for better comparability. Cre: creatine; Cit: citrate; Ala: alanine.

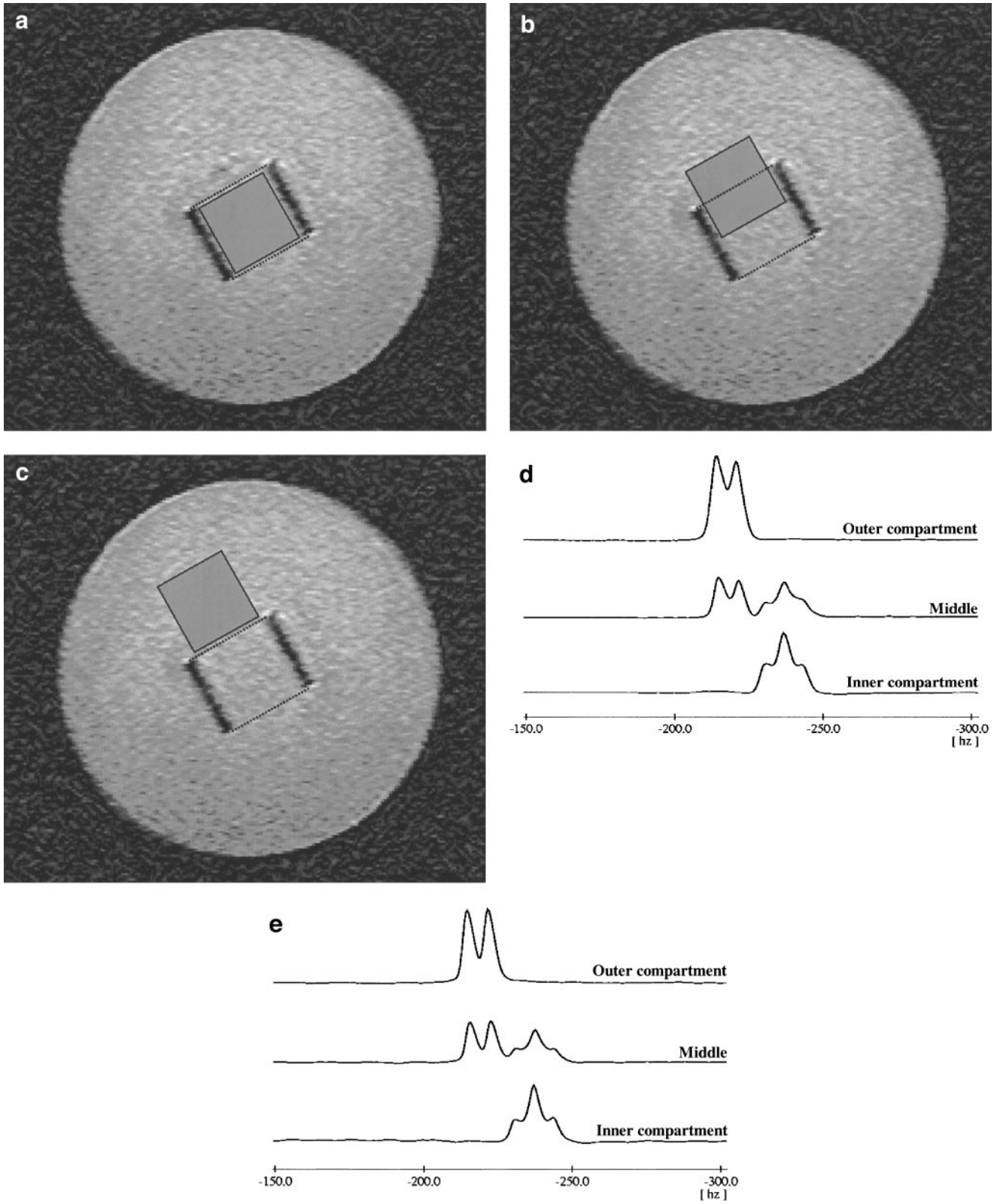

FIG. 9. Two-chamber phantom containing 100 mmol/L ethanol (inner compartment) and 100 mmol/L alanine (outer compartment). (a)–(c) Positions of the VOIs. (d) PRESS spectra (TE = 272 ms) acquired in the three VOIs depicted in (a)–(c). (e) Spectra acquired in the three VOIs depicted in (a)–(c) using a $[(\pi/2)_x-\tau-(\pi)_y-\tau-(\pi/2)_y-\tau-(\pi)_y-\tau-\text{acquire}]$ sequence ($t_1 = t_2 = \tau$; TE = 4τ = 272 ms). Dashed lines indicate position of the plastic foils separating the compartments.

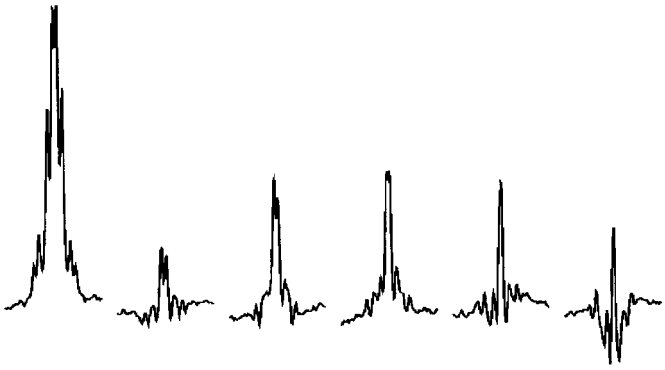

FIG. 10. Spectra of the taurine A_2B_2 spin system. From left to right: PRESS spectrum (TE = 30 ms), SQC filtered spectra ($t_1 = t_2 = \tau$; TE = 4τ = 60, 80, 100, 120, 140 ms).

cycle" phase cycle (*24*). In order to avoid signal arising from spins which see only the second ($\pi/2$) pulse, but not the first one (i.e., spins experiencing a $[(\pi/2)_x–t_2–(\pi)–t_2–$acquire] sequence), the used phase cycling scheme was designed in such a way that the phase of the second ($\pi/2$) pulse alternates throughout the phase cycling between x and $-x$ or y and $-y$, respectively.

Postprocessing consisted of direct current correction, zero-filling to 4096 complex points, and exponential filtering, resulting in a line broadening of 1.5 Hz.

RESULTS

SQC Filter Performance

Figures 6 and 7 show SQC filtered spectra of 2,4-dichloropyrimidine and trilithium citrate, respectively. The echo times TE = 4τ ($t_1 = t_2 = \tau$) range from 60 to 140 ms in both cases. For comparison, a short echo-time PRESS spectrum (TE = 30 ms; $TE_1 = TE_2 = 15$ ms) is shown.

As expected, a pronounced signal is obtained in the SQC filtered spectrum of the trilithium citrate AB spin system (Fig. 7). The dependence on the echo time is apparent. For the 2,4-dichloropyrimidine AX spin system (Fig. 6), the SQC filter yields only a considerably attenuated signal, which is still dependent on the echo time. This observable signal is not only due to experimental imperfections, but also stems from residual strong coupling effects (cf. Fig. 5).

Figure 8, which compares a short echo-time PRESS spectrum (TE = 30 ms; $TE_1 = TE_2 = 15$ ms) and a SQC filtered spectrum (TE = 4τ = 80 ms; $t_1 = t_2 = \tau$) of the mix phantom, demonstrates the selectivity of the sequence for strongly coupled spin systems. The two creatine resonances, which arise from uncoupled spin systems, as well as the resonances of the weakly coupled alanine spin system, are widely suppressed. For the strongly coupled citrate spin system the filter returns a clear signal.

Figure 9 shows the CH_3 region of the spectra obtained in the two-chamber phantom. The nominal VOI was placed in the inner compartment (Fig. 9a), on the parting line (Fig. 9b) or in the outer compartment, but close to the plastic foil separating the two compartments (Fig. 9c). For both, the PRESS sequence (Fig. 9d) and the $[(\pi/2)_x–\tau–(\pi)_y–\tau–(\pi/2)_y–\tau–(\pi)_y–\tau–$acquire] sequence (Fig. 9e), no visible contamination from outside the selected VOI is present.

Figure 10 displays signals of the taurine AA′BB′ spin system formed up by the SQC filtering sequence. A signal maximum for the SQC filter occurs at TE $\approx$ 80 ms, where the "observable" yield of the SQC filtering sequence (i.e., the signal amplitude of the taurine peak in the filtered spectrum compared to a spectrum recorded with a pulse–acquire sequence) is 40%. This echotime was used to record signals from phantoms containing choline and *myo*-inositol, respectively (Fig. 11). When comparing short echo-time PRESS spectra (Fig. 11a) with the filtered spectra, one notices considerable reduced contributions from choline and *myo*-inositol, while the taurine peak becomes sharper. However, residual signals arising from *myo*-inositol still heavily disturb the baseline in the spectral region of the taurine resonances.

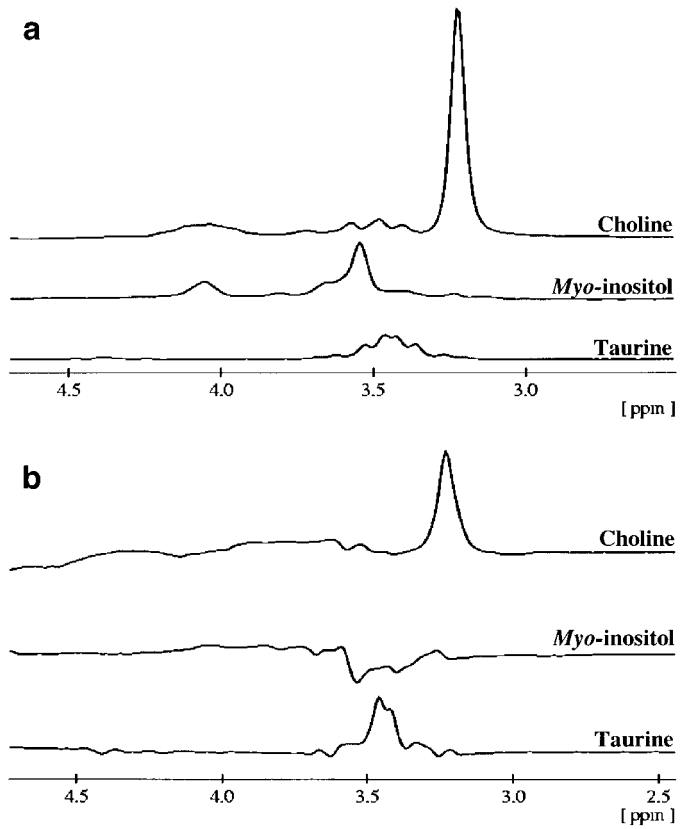

FIG. 11. (a) PRESS spectra (TE = 30 ms) of phantoms containing (top to bottom) 100 mmol/L choline, 100 mmol/L *myo*-inositol, and 100 mmol/L taurine. (b) SQC filtered spectra ($t_1 = t_2 = \tau$; TE = 4τ = 80 ms) of the same phantoms, vertical scale six times larger than in (a).

DISCUSSION

In the approach chosen in this paper, the proposed pulse sequence for localized NMR spectroscopy is treated as a special form of a MQC filter. The sequence consists of the same sequel of RF pulses as the *J*-refocused double spin echo experiment discussed in (*25, 26*). The latter experiment uses a $(\pi/2)_y$ pulse introduced to the double spin echo experiment at the time of the first echo top for inducing a homonuclear magnetization transfer. In the proposed SQC filter, the corresponding $(\pi/2)$ pulse induces a rotation along the *x*-axis and transforms SQC built up by uncoupled and weakly coupled spin systems into nonobservable longitudinal magnetization and MQC of even orders. On this basis, the single-quantum coherence filtering technique provides discrimination between strongly coupled spins on the one hand and uncoupled as well as weakly coupled spins on the other hand, as demonstrated in the *in vitro* experiments.

Singlet suppression is accomplished by creating longitudinal spin order by the second $(\pi/2)$ pulse. Thus, accurate calibration of the pulse phase is essential. However, the first experiments presented in this report suggest that the proposed calibration procedure, which proved itself to be useful for calibrating a DQC filter (*10*), is not sufficient to achieve a singlet suppression of a factor >100, as is possible with sequences that use dephasing gradients for this purpose. Allen *et al.* propose the use of self-refocusing pulses (*3*) for spectral editing sequences. These ensure that all terms in the density operator are in phase after a RF pulse (*3, 8*). Such pulses may contribute to far better suppression factors of unwanted signal of uncoupled spins. A second essential point is the integrity of the pulse angles. If the angle induced by the two refocusing pulses deviates from 180°, unwanted residual signals may be induced. These are removed by means of spoiler gradients around the refocusing pulses (cf. Fig. 2).

As the proposed spectral editing technique suppresses signal of spin systems which satisfy the weak coupling limit, the detected signal intensities are in principle a measure of the extent to which the weak coupling approximation is justifiable. The example of 2,4-dichloropyrimidine shows that for $\Delta\nu/J \cong 11$ residual strong coupling effects may be observed.

The application of the proposed sequence for the detection of taurine is only one example of a wide range of applications of SQC filters. For some spin systems it might be advantageous to make the second $(\pi/2)$ pulse frequency selective. In this way, magnetization transfer takes place only for the spin system of interest, whereas in other spin systems only coherence orders $\neq 1$ or longitudinal magnetization are excited.

Until now there have been only a few reports of *in vivo* detection of taurine in the human brain by means of proton NMR at the "standard" main field strength of 1.5 T. Hardy and Norwood (*28*) as well as Lei and Peeling (*29*) recently proposed double-quantum coherence filtering sequences for use at high fields (>3.5 T). Experiments at 1.5 T with a double-quantum coherence filtering sequence as described in (*10*) showed disappointing results in terms of signal yield (unpublished data).

Our preliminary results demonstrate that taurine might be detectable using the proposed SQC filtering sequence, considering the signal yield of 40% at a relatively short echo time of 80 ms. However, the suppression of the singlet arising from the trimethyl entity of choline-containing compounds at 3.23 ppm must be improved. The contamination of the taurine SQC signal with contributions of the strongly coupled *myo*-inositol spin system at 3.28 and 3.54 ppm was alleviated by the proper adjustment of the sequence timing.

The use of the proposed sequence is not restricted to a main field of 1.5 T. In quite a number of biomolecules (as, e.g., taurine), strong coupling effects should be also present at fields up to 4.7 T as used in animal scanners. The evolution of strongly coupled spin systems depends on the chemical shift differences between spins as well as on the scalar coupling constants. The former introduces a field dependence of the filter output. This means that the filter performance must be calculated for each main field used.

In conclusion, the proposed SQC filtering sequence promises to be a versatile tool for the selective localized *in vivo* detection of strongly coupled spin systems. The implementation on a whole-body scanner is straightforward, as it only requires the introduction of one additional pulse to the PRESS sequence. From the results presented in Fig. 9, we conclude that the localization properties are equal to those of the routinely used PRESS sequence (*1*).

ACKNOWLEDGMENT

This research was supported by Swiss National Science Foundation Grant 31-52173.97.

REFERENCES

1. P. A. Bottomley, Spatial localization in NMR spectroscopy *in vivo, Ann. N.Y. Acad. Sci.* **508,** 333–348 (1987).
2. J. Frahm and K. D. Merboldt, Localized proton spectroscopy using stimulated echoes, *J. Magn. Reson.* **72,** 502–508 (1987).
3. P. S. Allen, R. B. Thompson, and A. H. Wilman, Metabolite-specific NMR spectroscopy *in vivo, NMR Biomed.* **10,** 435–444 (1997).
4. R. B. Thompson and P. S. Allen, An integrated volume localization spectral editing pulse sequence, *in* "Proc., SMR, 3rd Annual Meeting," Nice, p. 1909 (1995).
5. L. Jouvensal, P. G. Carlier, and G. Bloch, Double quantum proton editing of lactate in the human calf during exercise with one-minute time resolution at 3T, *in* "Proc., SMR, 3rd Annual Meeting," Nice, p. 427 (1995).
6. L. Jouvensal, P. G. Carlier, and G. Bloch, Practical implementation of single-voxel double-quantum editing on a whole-body NMR spectrometer: Localized monitoring of lactate in the human leg during and after exercise, *Magn. Reson. Med.* **36,** 487–490 (1996).
7. J. R. Keltner, L. L. Wald, B. de B. Frederick, and P. F. Renshaw, *In*

vivo detection of GABA in human brain using a localized double-quantum filter technique, *Magn. Reson. Med.* **37,** 366–371 (1997).

8. R. B. Thompson and P. S. Allen, A new multiple quantum filter design procedure for use on strongly coupled spin systems found *in vivo:* Its application to glutamate, *Magn. Reson. Med.* **39,** 762–771 (1998).
9. J. R. Keltner, L. L. Wald, P. J. Ledden, Y. C. I. Chen, R. T. Matthews, E. H. G. K. Küestermann, J. R. Baker, B. R. Rosen, and B. G. Jenkins, A localized double-quantum filter for the *in vivo* detection of brain glucose, *Magn. Reson. Med.* **39,** 651–656 (1998).
10. A. H. Trabesinger, O.M. Weber, C. O. Duc, and P. Boesiger, Detection of glutathione in the human brain in vivo by means of double quantum coherence filtering, *Magn. Reson. Med.* **42,** 283–289 (1999).
11. G. C. McKinnon and P. Boesiger, Localized double-quantum filter and correlation spectroscopy experiments, *Magn. Reson. Med.* **6,** 334–343 (1988).
12. H. Sotak, D. M. Freeman, and R. E. Hurd, The unequivocal determination of *in vivo* lactic acid using two-dimensional double-quantum-coherence-transfers spectroscopy, *J. Magn. Reson.* **78,** 355–361 (1988).
13. A. Knüttel and R. Kimmich, Double-quantum filtered volume-selective NMR spectroscopy, *Magn. Reson. Med.* **10,** 404–410 (1989).
14. S. Crozier, I. M. Brereton, S. E. Rose, J. Field, G. F. Shannon, and D. M. Doddrell, Application of volume-selected, two-dimensional multiple-quantum editing *in vivo* to observe cerebral metabolites, *Magn. Reson. Med.* **16,** 496–502 (1990).
15. M. A. Thomas, H. P. Hetherington, D. J. Meyerhoff, and D. B. Twieg, Localized double-quantum-filtered ^{1}H NMR spectroscopy, *J. Magn. Reson.* **93,** 485–496 (1991).
16. R. R. Ernst, G. Bodenhausen, and A. Wokaun, "Principles of Nuclear Magnetic Resonance in One and Two Dimensions," Oxford Univ. Press, Oxford (1991).
17. A. Bax, P. G. De Jong, A. F. Mehlkopf, and J. Smidt, Separation of the different orders of NMR multiple-quantum transitions by the use of pulsed field gradients, *Chem. Phys. Lett.* **69,** 567–570 (1980).
18. O. W. Sørensen, G. W. Eich, M. H. Levitt, G. Bodenhausen, and R. R. Ernst, Product operator formalism for the description of NMR pulse experiments, *Prog. NMR Spectrosc.* **16,** 163–192 (1983).
19. K. J. Pecker, and K. M. Wright, The use of a single-spin operator basis set in the NMR spectroscopy of scalar-coupled spin systems, *Mol. Phys.* **50,** 797–813 (1983).
20. F. J. M. Van DeVen, and C. W. Hilbers, A simple formalism for the description of multiple-pulse experiments. Application to a weakly coupled two-spin ($I = \frac{1}{2}$) system, *J. Magn. Reson.* **54,** 512–520 (1983).
21. L. E. Kay and R. E. D. McClung, A product operator description of AB and ABX spin systems, *J. Magn. Reson.* **77,** 258–273 (1988).
22. C. E. Wright, H. H. Tallan, Y. Y. Lin, and G. E. Gaull, Taurine: Biological update, *Annu. Rev. Biochem.* **55,** 427–453 (1986).
23. R. W. Chesney, Taurine: Its biological role and clinical implications, *Adv. Pediatr.* **32,** 1–42 (1985).
24. G. Bodenhausen, R. Freeman, and D. L. Turner, Suppression of artifacts in two-dimensional *J* spectroscopy use, *J. Magn. Reson.* **27,** 511–514 (1977).
25. K. Takegoshi, K. Ogura, and K. Hikichi, A perfect spin echo in a weakly homonuclear *J*-coupled two spin-$\frac{1}{2}$ system, *J. Magn. Reson.* **84,** 611–615 (1989).
26. P. C. M. van Zijl, C. T. W. Moonen, and M. von Kienlin, Homonuclear *J* refocusing in echo spectroscopy, *J. Magn. Reson.* **89,** 28–37 (1990).
27. H. Geen and R. Freeman, Band-selective radiofrequency pulses, *J. Magn. Reson.* **93,** 93–141 (1991).
28. D. L. Hardy and T. J. Norwood, Spectral editing technique for the *in vivo* and *in vitro* detection of taurine, *J. Magn. Reson.* **133,** 70–78 (1998).
29. H. Lei and J. Peeling, A localized double-quantum filter for in vivo detection of taurine, *Magn. Reson. Med.* **42,** 454–460 (1999).